



Numerical Simulation of Laminar Flow and Heat Transfer of Waxy Oil with Yield Stress in a Pipe with Sudden Enlargement

Uzak Zhabbasbayev,^{1,2} Timur Bekibayev,^{1,2,*} Maksim Pakhomov³ and Zhibek Akasheva^{1,*}

Abstract

This study investigates the non-isothermal laminar flow and heat transfer of waxy oil in a pipe with a sudden enlargement, emphasizing its transition from a Newtonian to a viscoplastic state during cooling. Using the Schwedoff-Bingham rheological model, the motion and heat transfer governing equations were numerically solved via Patankar's control volume method in "velocity components-pressure" variables. A significant transformation is observed in the flow structure. In isothermal conditions with Reynolds numbers of 1046 and 2092 and Bingham numbers of 0.05 and 0.025, reverse flow zones and negative pressure distributions are observed. However, under non-isothermal conditions with Bingham numbers ranging from 8.5 to 59.14, reverse flow zones disappear, replaced by a stagnation zone with zero velocity due to increased plastic viscosity and yield stress during oil cooling. The study also demonstrates an enhanced convective heat transfer arising from the sudden pipe enlargement. The novelty of this work lies in its focus on the temperature-dependent rheological transformation of waxy oil, extending beyond previous studies by providing detailed insights into the interplay between flow structure and thermal effects in viscoplastic fluids. These findings are critical for optimizing pipeline operations and ensuring efficient transport of waxy oils.

Keywords: Laminar flow; Heat transfer; Waxy oil; Yield stress; Schwedoff-Bingham model; Patankar's numerical method.

Received: 08 November 2024; Revised: 12 December 2024; Accepted: 15 December 2024.

Article type: Research article.

1. Introduction

Modeling fluid movement in pipes with variable radii is important for studying the characteristics of liquid media transporting and processing materials, such as pastes, paints, polymer melts, and petroleum products, in technical applications under certain conditions. Suddenly, expanding elements in pipes make it possible to control flow and plan loads on the pipeline and pressure distribution. The flow of Newtonian fluid in pipes with sudden enlargement under various conditions and radius ratios of the pipe sections has been widely studied numerically and experimentally.^[1-3]

Modeling many technological processes is accompanied by the need to study the flow of non-Newtonian fluids.^[4-9] The

movement of a fluid is considered to obey a power law in pipes with a variable cross-sectional area.^[10,11] These flows consist of the following structural parts: regions near the inlet and outlet sections - one-dimensional flow zones; regions upstream and downstream from the cross-sectional change - two-dimensional flow zones; and a region with circulating flow near the internal corner - the circulation zone. The lengths of these zones differ depending on the Reynolds number.

Among the studies focused on fluid movement in pipes with sudden enlargement, significant attention is given to determining the length of the circulation zone,^[12,13] and examining the conditions under which the flow symmetry is disrupted.^[14] Hammad studied the following flow pattern near the pipe enlargement and observed that the flow divides at the point of sudden enlargement, with the main flow continuing along the pipe axis while a circulation zone forms near the internal corner.^[13] The distance from the cross-sectional change to the place where the main flow joins the solid boundary determines the length of the circulation zone. The presence of enlargement in pipes promotes flow mixing due to the formation of a circulation zone after the cross-sectional change. For example, a sequence of sudden enlargements was

¹ Laboratory "Modeling in Energy Sector", Satbayev University, Almaty, 050013, Kazakhstan

² U.A. Joldasbekov Institute of Mechanics and Engineering, Almaty, 050000, Kazakhstan

³ Laboratory "Thermogasdynamics", Kutateladze Institute of Thermophysics SB RAS, Novosibirsk, 630000, Russia

*Email: timur_bekibaev@mail.ru (T. Bekibayev),

akasheva.zhibek@gmail.com (Z. Akasheva)

used to improve the mixing of reagents in a reactor designed to remove crystalline phosphorus from wastewater.^[15] In another case, the isothermal flow of a power-law fluid was considered in a pipe with symmetrical sudden enlargement of 1:2 for a Reynolds number of $Re=10$.^[16] The length of the circulation zone is observed to depend on the nonlinearity index.

The enlargement rate of a pipe is also used as a determining parameter for flow characteristics. An increased length of the circulation zone is displayed as the degree of enlargement increases.^[17–20] The study shows how the stream function isolines change for the fluid flow obeying the power law in a flat pipe as the Reynolds number (Re) varies from 40 to 130.^[21] For various degrees of fluid nonlinearity, the Re values that lead to disruption of the flow symmetry are determined.

As a result of studies on the fluid movement in a pipe with sudden enlargement, local pressure losses were determined, arising from the sudden change in the flow region geometry. A review of the work includes information on the calculated results of local hydraulic pressure losses for pipes with varying degrees of enlargement in studying the flow of non-Newtonian fluids.^[22] Mamazova *et al.*^[23] present experimental studies of the viscoplastic fluid flow structure characteristics in a pipe with enlargement for various Re values.

Heat transfer processes of laminar flow were studied in a pipe with enlargement.^[24–28] The non-isothermal laminar flow of Bingham fluid was investigated in a pipe with sudden enlargement.^[24–26] The results establish flow and heat transfer patterns for non-Newtonian fluids that differ from those observed in Newtonian fluids. In both with and without circulation zones, the thermal convection of viscoplastic fluids is considered in a pipe with enlargement.^[27] In parametric calculations, the effects of geometry, inertia, rheology, and thermophysical properties on the structure of thermal convection are found. The steady laminar flow of a viscoplastic fluid with Herschel-Bulkley rheology was investigated under non-isothermal conditions with sudden pipe narrowing.^[28] The parametric calculations reveal non-deformable zones within the flow region.

In this work, unlike in well-known studies, the plastic viscosity $\mu_p(t)$ and the yield stress $\tau_0(t)$ of a viscoplastic fluid are temperature-dependent, allowing for an analysis of how mode parameters influence the structure of flow and heat transfer in a pipe with a sudden enlargement.

2. Mathematical model

2.1 Physical formulation

A non-isothermal viscoplastic non-Newtonian fluid of waxy crude oil flows in a pipe with a sudden enlargement (Fig. 1). The sudden enlargement of the pipe leads to the formation of a circulation zone, which influences the mass and heat transfer processes, described by the distribution of velocity, pressure, and temperature.

The diameter of a pipe before a sudden enlargement is $D_1=2R_1=0.05$ m, the step height is $H=0.01$ m, the average

velocity at the pipe inlet varies within the range of $u_1=0.05\div 0.20$ m/s, the average inlet temperature is $t_1=25$ °C. The Re is determined by the flow parameters at the pipe inlet and varies within the range of $Re=\rho_1 2R_1 u_1 / \mu_{p1} = 523/2092$. The ratio of the pipe diameters to the inlet diameter is given by $ER=(R_2/R_1)^2=1.96$. The temperature of the pipe wall varies within the range of $t_w=5/25$ °C. The wall temperature determines the Bingham number $Bn=\tau_{0w} 2R_1 / (\mu_{pw} u_1)$, which varies from 0.02534 to 59.14. The density of fluid flow in the inlet cross-section is $\rho_1=850$ kg/m³. The Prandtl number (Pr) is 45.

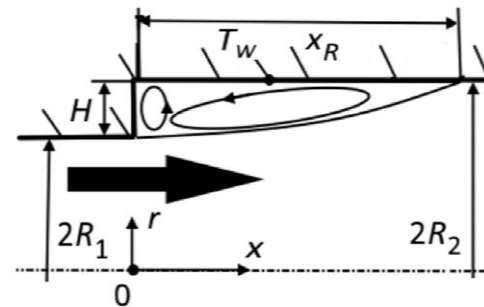


Fig. 1: Flow diagram in a pipe with a sudden enlargement.

2.2 Rheology of viscoplastic fluid

The rheology of waxy oil can be modeled using the Schvedoff-Bingham fluid model. Then, the effective molecular viscosity of the fluid μ_{eff} is expressed by equation (1):^[29–31]

$$\mu_{eff} = \begin{cases} \mu_p + \tau_0 |\dot{\gamma}|^{-1}, & \text{if } |\tau| > \tau_0 \\ \infty, & \text{if } |\tau| \leq \tau_0 \end{cases} \quad (1)$$

where τ_0 is the yield stress, and μ_p is the plastic viscosity, $|\tau| = \sqrt{\tau_{ij}\tau_{ij}}$, $\dot{\gamma} = \sqrt{2S_{ij}S_{ij}} = S$, $S_{ij} = 0.5 \left(\frac{\partial U_i}{\partial x_j} + \frac{\partial U_j}{\partial x_i} \right)$.

The main difficulty in numerical modeling of viscoplastic flows arises from the existence of singular molecular viscosity in regions where the shear stress is less than τ_0 . To regulate expression (1), equation (2) is used:^[32]

$$\mu_{eff} = \mu_p + \tau_0 \frac{[1 - \exp(-10^3 |\dot{\gamma}|)]}{|\dot{\gamma}|} \quad (2)$$

2.3 The governing equations

The system of equations of motion and heat transfer of a viscoplastic fluid in a cylindrical coordinate system in dimensionless variables can be written as:

$$\frac{\partial U}{\partial \bar{x}} + \frac{1}{\bar{r}} \frac{\partial}{\partial \bar{r}} (\bar{r}V) = 0 \quad (3)$$

$$U \frac{\partial U}{\partial \bar{x}} + V \frac{\partial U}{\partial \bar{r}} = -\frac{\partial P}{\partial \bar{x}} + \frac{1}{Re} \left[\frac{\partial}{\partial \bar{x}} \left(2\mu_{eff} \frac{\partial U}{\partial \bar{x}} \right) + \frac{1}{\bar{r}} \frac{\partial}{\partial \bar{r}} \left(\mu_{eff} \bar{r} \left(\frac{\partial U}{\partial \bar{r}} + \frac{\partial V}{\partial \bar{x}} \right) \right) \right] \quad (4)$$

$$U \frac{\partial V}{\partial \bar{x}} + V \frac{\partial V}{\partial \bar{r}} = -\frac{\partial P}{\partial \bar{r}} + \frac{1}{Re} \left[\frac{\partial}{\partial \bar{x}} \left(\mu_{eff} V \left(\frac{\partial V}{\partial \bar{x}} + \frac{\partial U}{\partial \bar{r}} \right) \right) - \frac{2\mu_{eff} V}{\bar{r}^2} + \frac{1}{\bar{r}} \frac{\partial}{\partial \bar{r}} \left(2\bar{r} \mu_{eff} \frac{\partial V}{\partial \bar{r}} \right) \right] \quad (5)$$

$$\frac{\partial (\bar{c}_p U \theta)}{\partial \bar{x}} + \frac{\partial (\bar{c}_p V \theta)}{\partial \bar{r}} = \frac{1}{Pe} \left[\frac{\partial^2 \theta}{\partial \bar{x}^2} + \frac{1}{\bar{r}} \frac{\partial}{\partial \bar{r}} \left(\bar{r} \frac{\partial \theta}{\partial \bar{r}} \right) \right] + \frac{Br}{Pe} \Phi(\bar{x}, \bar{r}) \quad (6)$$

where $\bar{x} = \frac{x}{R}$, $\bar{r} = \frac{r}{R}$, $U = \frac{u}{u_1}$, $V = \frac{v}{u_1}$, $P = \frac{p}{\rho u_1^2}$, $\theta = \frac{(t-t_w)}{(t_1-t_w)}$, $\bar{c}_p = c_p(t)/c_{p1}$, Re , Pe , Bn are Reynolds, Peclet, and

Brinkman numbers, respectively; and $\Phi(\bar{x}, \bar{r})$ is the dissipation function.

The dependences of the coefficients of plastic viscosity $\mu_p(t)$, yield stress $\tau_0(t)$, and heat capacity $c_p(t)$ on temperature are given in the study.^[33]

2.4 Boundary conditions

The following conditions are set on the pipe wall:

$$\bar{r} = 1, U = V = \theta = 0 \tag{7}$$

The following conditions are set on the pipe axis:

$$\bar{r} = 0, \frac{\partial U}{\partial \bar{r}} = \frac{\partial V}{\partial \bar{r}} = \frac{\partial \theta}{\partial \bar{r}} = 0 \tag{8}$$

At the pipe inlet, the conditions are set:

$$\bar{x} = 0: U=1, V=0, \theta = 1, \tag{9}$$

At the pipe outlet, the conditions are set:

$$\bar{x} = L/R: \frac{\partial U}{\partial \bar{x}} = \frac{\partial V}{\partial \bar{x}} = \frac{\partial \theta}{\partial \bar{x}} = 0 \tag{10}$$

The dependence of plastic viscosity $\mu_p(t)$ and yield stress $\tau_0(t)$ on the temperature of waxy oil is determined by experimental data and is given in Table 1.

Table 1: The dependence of yield shear stress and plastic viscosity of non-Newtonian fluid.

t, °C	T, K	τ_0 , Pa	μ_p , Pa·s
0	273	589.6	0.3585
5	278	34.62044	0.14634
10	283	2.03286	0.05974
15	288	0.11937	0.02438
20	293	0.00701	0.00995
25	298	4.1156E-4	0.00406
30	303	2.41662E-5	0.00166

2.5 Numerical realization

Systems of two-dimensional Navier–Stokes equations are solved using a pressure correction procedure. In the “predictor” step, preliminary velocities are determined for a frozen pressure field while solving the equations of fluid motion. Next, in the “corrector” step, the pressure correction field is calculated to satisfy the continuity equation in each grid cell, followed by corrections to the velocity and pressure fields. A characteristic feature of the algorithm involves constructing discretization schemes for the original equations based on the increments of the dependent variables. In this approach, the finite-volume approximation of the original differential equation is placed in the explicit part of the equations, particularly in the momentum equations. In the implicit part, a simplified form of the same equation is expressed concerning the increments of dependent variables, supplemented by stabilizing terms. The resulting intermediate velocity field is obtained for a given pressure distribution, though it does not satisfy the continuity equation. Consequently, it is necessary to introduce a pressure correction in each grid cell so that the corrected velocity field, accounting for this adjustment, satisfies the continuity equation.^[34]

The relationship between velocity $\delta \vec{V}$ and pressure δP corrections has the form:

$$a_p \delta \vec{V}_p = \sum_{w,e,s,n} a_{nb} \delta \vec{V}_{nb} - \sum_{w,e,s,n} \delta P \Delta \vec{s} \tag{11}$$

The finite volume method on the staggered grid discretized the equations. The semi-implicit method for pressure-linked equations (SIMPLE) algorithm was used to solve the different equations of the Navier-Stokes system.^[34]

2.6 Verification of the numerical method

Fig. 2 compares the calculated data with the experimental results from the literature to determine the length of the reverse flow zone in a pipe with a sudden enlargement.^[31] The points are the numerical simulation results for the laminar non-Newtonian fluids of the study, and the curves are the authors’ predictions for $ER=(R_2/R_1)^2=4$. As seen from Fig. 2, the calculated relationships between the length of the reverse flow zone and the Bingham number at various Reynolds numbers align with the experimental data of the study.^[35]

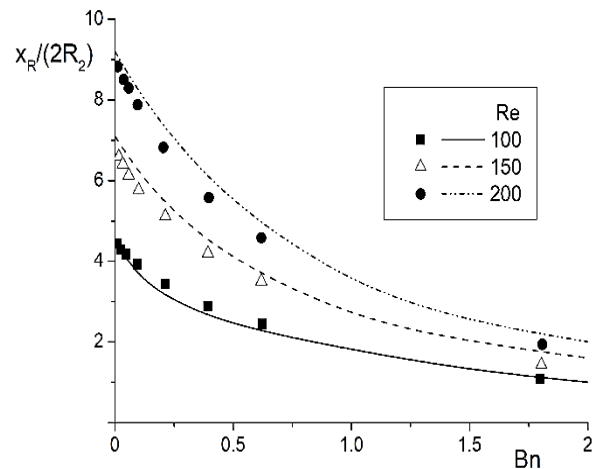


Fig. 2: The effect of Reynolds numbers $Re=\rho_1 2R_1 u_1 / \mu_{p1}$ on the circulation length x_R for various values of Schwedoff-Bingham fluids $Bn=\tau_{0w} 2R_1 / (\mu_{pw} u_1)$.

Fig. 3 illustrates the distribution of the heat transfer enhancement coefficient for the Schwedoff-Bingham fluid along the length of a pipe with a sudden enlargement. The points are the numerical simulation for the laminar non-Newtonian fluids of the study,^[21] and the curves are the authors’ predictions for $Re=\rho_1 2R_1 u_1 / \mu_{p1}=100$, $Pr=\mu_p c_{p1} / \lambda_1=7$, and $ER=(R_2/R_1)^2=25$. Nu_{fd} is the Nusselt number for a fully developed flow in a pipe without a sudden enlargement.

As shown in Fig. 3, for the Bingham number of $Bn=0$ (Newtonian fluid), there is a good agreement between the calculation results and the data from the literature. For Bingham numbers of $Bn=1$ and $Bn=5$, the calculation results show slight discrepancies within the reverse flow zone. However, outside this zone, the calculations align closely with the data reported in the literature.^[21]

A comparison of the calculations for laminar motion and heat transfer of a viscoplastic fluid in a pipe with a sudden enlargement with data from other authors demonstrates the reliability of the numerical method used to solve the problem.

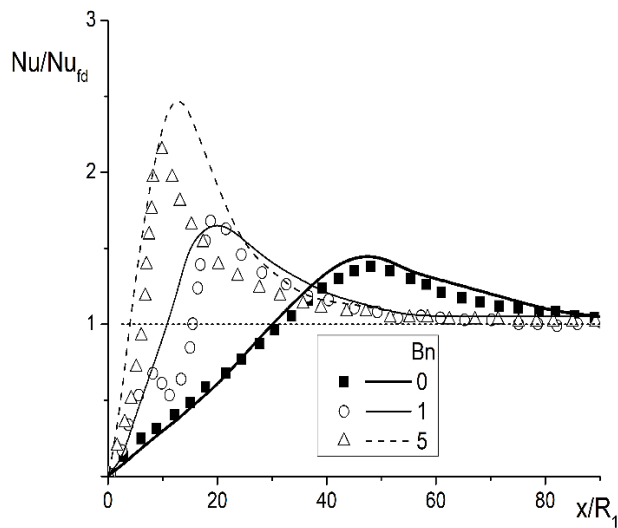


Fig. 3: The heat transfer enhancement ratio distributions Nu/Nu_{fd} along the pipe length for various values of Schwedoff-Bingham fluids $Bn = \tau_{0w} 2R_1 / (\mu_{pw} u_1)$.

3. Results and discussion

3.1 Isothermal laminar flow

The isothermal flow was simulated with the inlet flow temperature of $t_1 = 25\text{ }^\circ\text{C}$ and the wall temperature of $t_w = 25\text{ }^\circ\text{C}$ in the pipe with sudden enlargement. Fig. 4 shows the velocity vector contours of an isothermal flow at $Re = 1046$ and $Re = 2092$ and $Bn = 0.05$ and $Bn = 0.025$ in a pipe with a sudden enlargement.

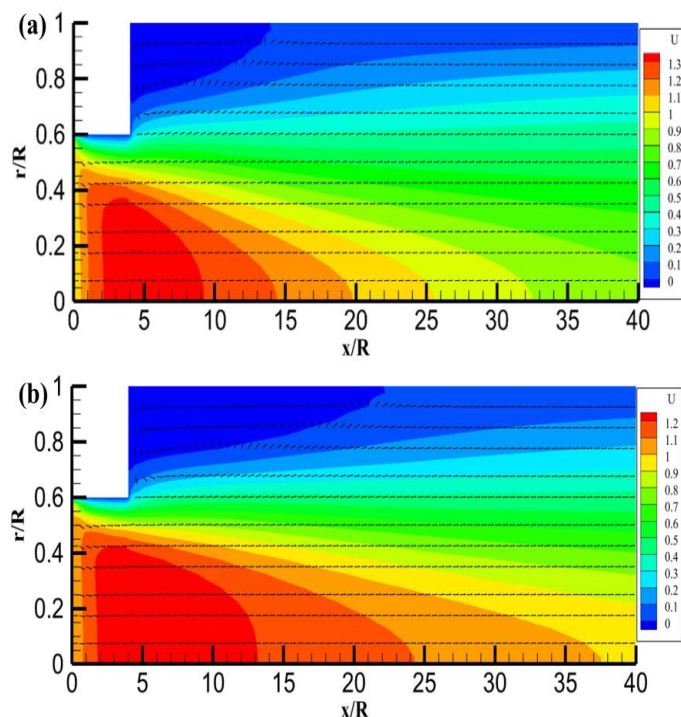


Fig. 4: Contours of the velocity vector of an isothermal flow in a pipe with a sudden enlargement at operating parameters: (a) $Re=1046$, $Bn=0.05068$; (b) $Re=2092$, $Bn=0.02534$.

The zone of reverse flows of viscoplastic fluid at $Re=1046$ and $Bn=0.05$ has a length from $x/R=4$ to $x/R=14$ (see Fig. 4a),

and at $Re=2092$ and $Bn=0.025$ has a length from $x/R=4$ to $x/R=24$ (see Fig. 4b).

The contours of the velocity vector show areas of maximum velocity values in the cross sections of a pipe with a sudden enlargement. In the case of $Re=1046$ and $Bn=0.05068$, the region of maximum value reaches the pipe section $x/R=9.3$ along the length, and for the case of $Re=2092$ and $Bn=0.02534$, the region of maximum value is up to the pipe section $x/R=13.2$. The sudden enlargement of a pipe cross-section causes a velocity increase and, accordingly, a pressure decrease. An increase in the Reynolds number of $Re=2092$ and a reduction in the Bingham number of $Bn=0.025$ increase the length of circulation zone, as shown in Fig. 4b.

Fig. 5 shows an isothermal flow's radial and axial velocity profiles at Reynolds numbers of $Re=1046$ and $Re=2092$ and the Bingham numbers of $Bn=0.05$ and $Bn=0.025$ in a pipe with a sudden enlargement. Radial profiles of the axial velocity in an isothermal flow clearly illustrate the influence of Reynolds and Bingham numbers on the flow structure in a pipe with a sudden enlargement.

As shown in Fig. 5a, the radial profiles of the axial velocity of an isothermal flow reveal reverse flows in the section $x/R=10$ of a pipe with a sudden enlargement. Additionally, the radial profiles of the axial velocity have a parabolic shape of the fluid flow in a pipe. As the Re increases to 2092, the reverse flow zone grows along the pipe length and radius. The radial profiles of the axial velocity up to the section $x/R=20$ have negative values near the pipe wall (see Fig. 5b).

Fig. 6 shows the pressure distribution of an isothermal flow at Re of 1046 and 2092 and the Bn of 0.05 and 0.025 along the length of a pipe with a sudden enlargement.

As shown in Fig. 6a, the pipe inlet pressure decreases and becomes negative, reaching a minimum value at the pipe section $x/R=4$. Subsequently, the pressure begins to increase, becoming positive at the pipe section $x/R=15$, where it reaches a maximum value before monotonically decreasing toward the pipe outlet. A sudden enlargement of a pipe's cross-section results in an increase in the kinetic energy of the fluid flow and a corresponding pressure drop. It is known that in subsonic flows, pressure disturbances propagate upstream, which explains the decrease in pressure in the inlet section, reaching a negative value before the sudden enlargement of a pipe. The minimum negative pressure value occurs at the pipe section $x/R=4$, where the cross-section change takes place. Beyond this point, the pressure increase causes the flow separation in the flow enlargement section and the formation of a reverse flow zone. At Re of 2092 and Bn of 0.02534, there is an observed increase in the minimum negative pressure value at the pipe section $x/R=4$ (Fig. 6b). The negative pressure value extends up to the section $x/R=35$, after which the pressure begins to recover toward the pipe outlet section.

3.2 Non-isothermal laminar flow and heat transfer

The non-isothermal flow was simulated for different values of the inlet flow temperature t_1 and the wall temperature t_w of a

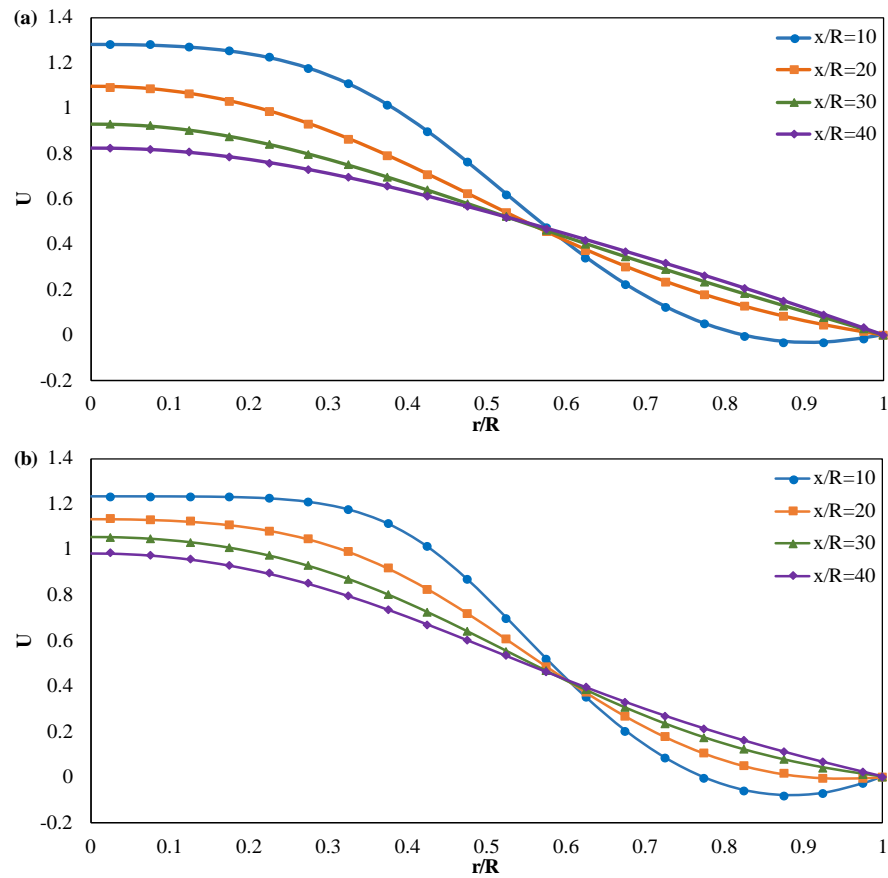


Fig. 5: Radial, axial velocity profiles of an isothermal flow in a pipe with a sudden enlargement at operating parameters: (a) $Re=1046$, $Bn=0.05068$; (b) $Re=2092$, $Bn=0.02534$.

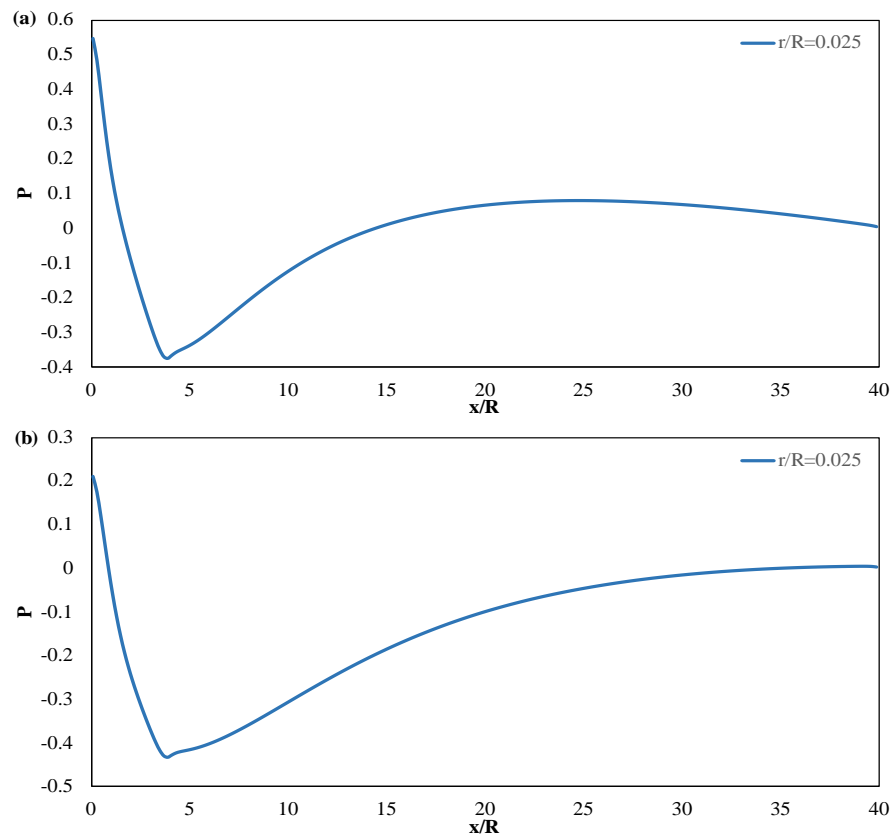


Fig. 6: Pressure distribution along the length of a pipe with a sudden enlargement at operating parameters: (a) $Re=1046$, $Bn=0.05068$; (b) $Re=2092$, $Bn=0.02534$.

pipe with a sudden enlargement. The Re is determined by the value of the plastic viscosity $\mu_p(t)$ at the inlet flow temperature, while the values of the plastic viscosity $\mu_{pw}(t_w)$ and yield stress $\tau_{0w}(t_w)$ at the pipe wall temperature determine the Bn . Fig. 7 illustrates the velocity vector contours at the inlet flow temperature of $t_1=25\text{ }^\circ\text{C}$, wall temperature of $t_w=5\text{ }^\circ\text{C}$, Reynolds numbers of $Re=1046$ and $Re=2092$, and Bingham numbers of $Bn=0.05$ and $Bn=0.025$ in a pipe with a sudden enlargement. The inlet flow temperature of $t_1=25\text{ }^\circ\text{C}$ begins to decrease due to the heat exchange between the waxy oil and the pipe wall, increasing the plastic viscosity $\mu_p(t)$ and the yield stress within the flow field.

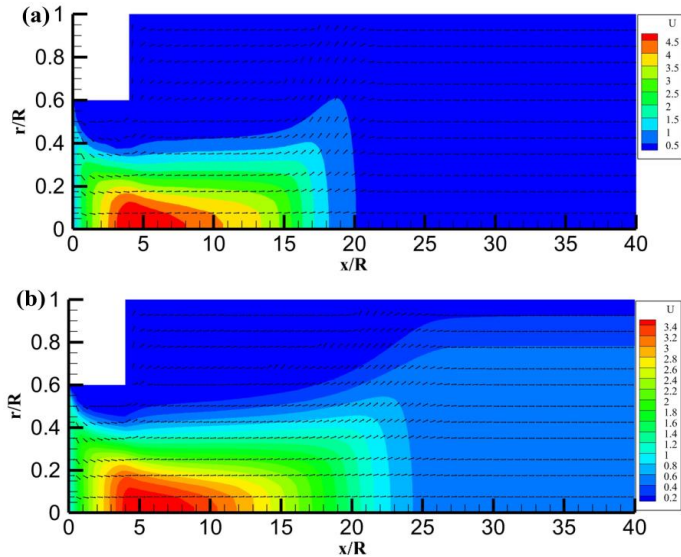


Fig. 7: Contours of the velocity vector in a pipe with a sudden enlargement at operating parameters: $t_1=25\text{ }^\circ\text{C}$, $t_w=5\text{ }^\circ\text{C}$, (a) $Re=1046$, $Bn=59.14$, (b) $Re=2092$, $Bn=29.57$.

As shown in Fig. 7, there are no reverse flows, and an extensive stagnation zone appears where the flow velocity is zero. The appearance of this stagnation zone is associated with the distribution of the yield stress $\tau_0(t)$ and plastic viscosity $\mu_p(t)$ in the flow field due to the decrease in fluid temperature. In this region, the fluid exists in a viscoplastic state. Additionally, the zone of the maximum velocity vector is reduced in the flow field, indicating a compression of the region where the maximum velocity occurs.

Fig. 8 demonstrates the radial profiles of axial velocity U and excess temperature θ in a pipe with a sudden enlargement at the inlet flow temperature of $t_1=25\text{ }^\circ\text{C}$, wall temperature of $t_w=5\text{ }^\circ\text{C}$, Reynolds number of $Re=1046$, and Bingham number of $Bn=59.14$.

As shown in Fig. 8a, the radial profiles of axial velocity clearly illustrate the movement of a viscoplastic fluid in a pipe with a sudden enlargement. In the pipe section $x/R=10$, the braking zone occupies a radius from $r/R=0.52$ to $r/R=1.0$. This leads to a reduction in the flow's cross-sectional area and an elongated axial velocity shape, with a maximum value on the pipe axis of $U_m=4.15$. After the braking zone, the radial profiles of the axial velocity begin to resemble those of Bingham fluid flow, characterized by a constant core in the axial region. Such forms are evident in the radial profiles of the axial velocity in the pipe sections from $x/R=20$ to $x/R=40$. It should be noted that the axial velocity profiles have areas of non-deformable (solid) body along the pipe length from $x/R=20$ to $x/R=40$. As shown in Fig. 8b, the excess temperature profiles θ decrease and equalize with the wall temperature. The enlargement of a pipe leads to a radial convective transfer of heat flux and an increase in the reduction of excess temperature θ along the pipe length.

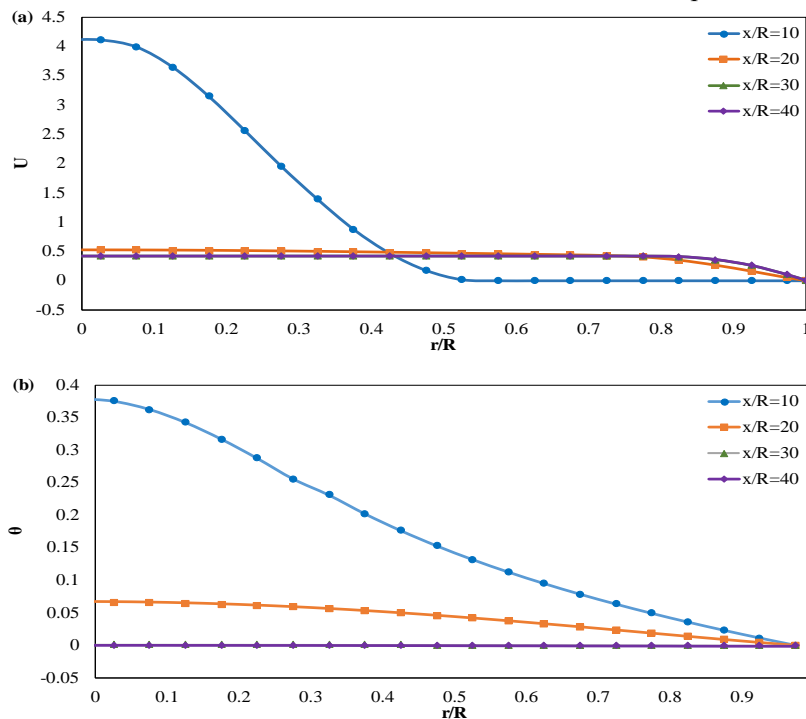


Fig. 8: Radial profiles of axial velocity U (a) and excess temperature θ , (b) in a pipe with a sudden enlargement at operating parameters: $t_1=25\text{ }^\circ\text{C}$, $t_w=5\text{ }^\circ\text{C}$, $Re=1046$, $Bn=59.14$.

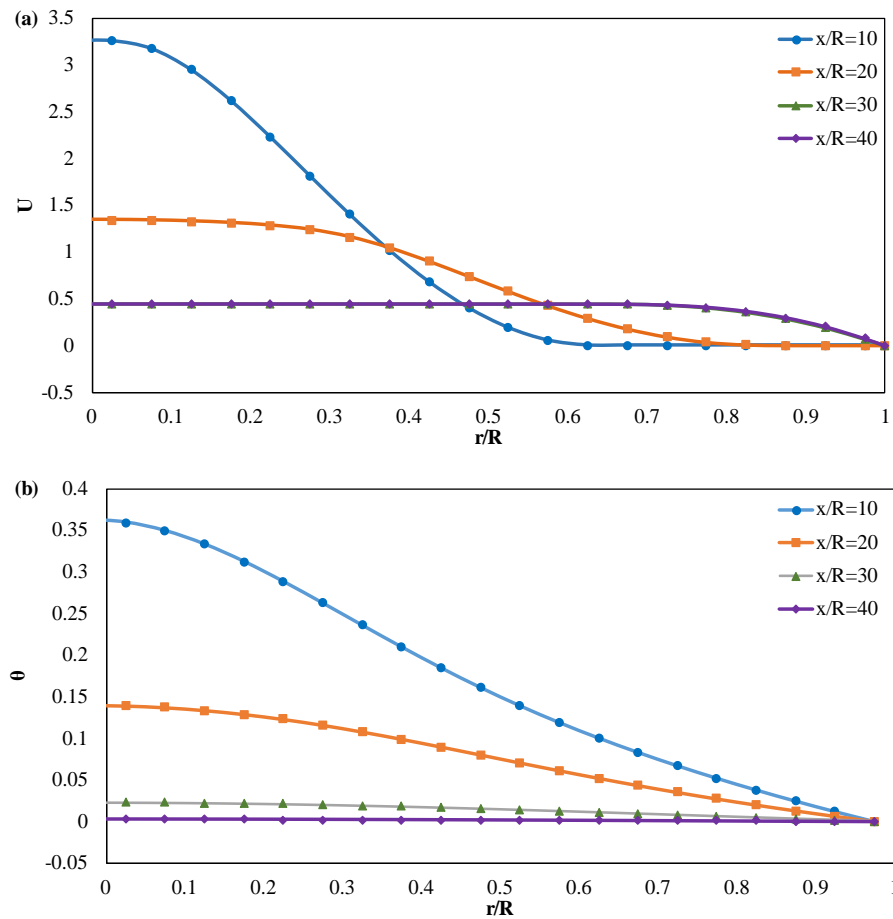


Fig. 9: Radial profiles of axial velocity U (a) and excess temperature θ (b) in a pipe with sudden enlargement at operating parameters: $t_1=25\text{ }^\circ\text{C}$, $t_w=5\text{ }^\circ\text{C}$, $Re=2092$, $Bn=29.57$.

Fig. 9 illustrates the radial profiles of axial velocity U and excess temperature θ at the inlet flow temperature of $t_1=25\text{ }^\circ\text{C}$, wall temperature of $t_w=5\text{ }^\circ\text{C}$, Reynolds number of $Re=2092$, and Bingham number of $Bn=29.57$ in a pipe with a sudden enlargement.

The stagnation zone in the pipe section $x/R=10$ extends from $r/R=0.57$ to $r/R=1.0$. Following the stagnation zone, the radial profiles of the axial velocity resemble those of a Bingham fluid flow (see Fig. 9a). In this mode, the increase in the Reynolds number of $Re=2092$ enhances the convective heat transfer and influences the distributions of the radial profiles of excess temperature in a pipe with a sudden enlargement (see Fig. 9b).

Fig. 10 shows the pressure distributions along the length of a pipe with a sudden enlargement at the inlet flow temperature of $t_1=25\text{ }^\circ\text{C}$, wall temperature of $t_w=5\text{ }^\circ\text{C}$, Reynolds numbers of $Re=1046$ and $Re=2092$, and Bingham numbers of $Bn=59.14$ and $Bn=29.57$.

As shown in Fig. 10a, at $Re=1046$ and $Bn=59.14$, the dimensionless pressure at the pipe inlet is $P=435$ (corresponding to $p=3697.5\text{ Pa}$), which decreases slightly in the pipe section $x/R=4$ and monotonically drops to the pipe outlet section $x/R=40$. The dimensionless pressure P exhibits a similar trend at $Re=2092$ and $Bn=29.57$ (see Fig. 10b). The high inlet pressure values are explained by the viscoplastic

state of the fluid in a pipe with sudden enlargement.

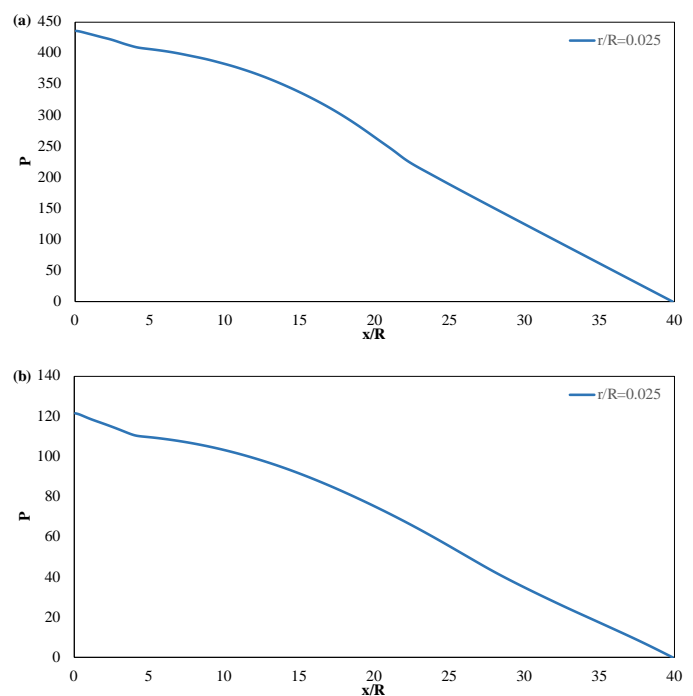


Fig. 10: Pressure distribution along the length of a pipe with a sudden enlargement at operating parameters: $t_1=25\text{ }^\circ\text{C}$, $t_w=5\text{ }^\circ\text{C}$; (a) $Re=1046$, $Bn=59.14$; (b) $Re=2092$, $Bn=29.57$.

Fig. 11 demonstrates the velocity vector contours at the inlet flow temperature of $t_1=25\text{ }^\circ\text{C}$, wall temperature of $t_w=10\text{ }^\circ\text{C}$, Reynolds numbers of $Re=1046$ and $Re=2092$, and Bingham numbers of $Bn=17.01$ and $Bn=8.5$ in a pipe with a sudden enlargement. The temperature of the pipe wall with sudden enlargement is $t_w=10\text{ }^\circ\text{C}$, and the temperature drop is less than that in the previous case (see Fig. 7). The sudden enlargement of a pipe increases the heat exchange between the flow and the wall, equalizing the flow temperature over the pipe cross-section.

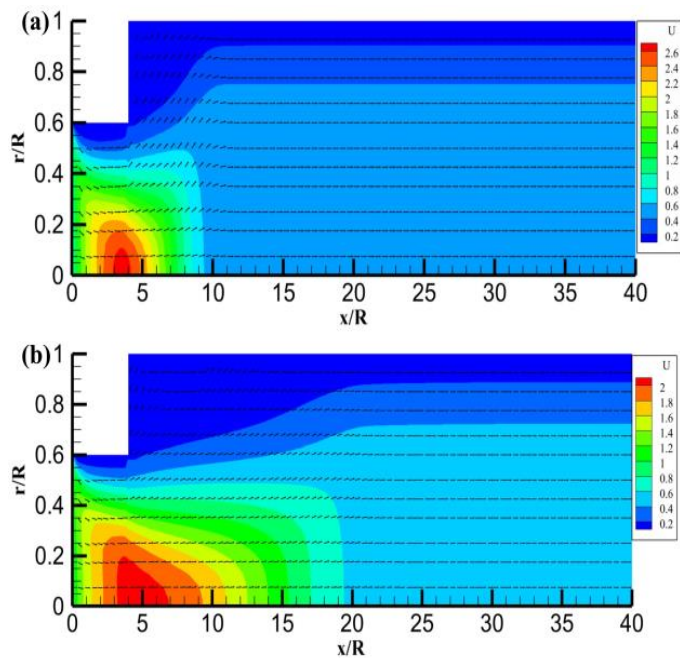


Fig. 11: Velocity vector contours along the length of a pipe with a sudden enlargement at operating parameters: $t_1=25\text{ }^\circ\text{C}$, $t_w=10\text{ }^\circ\text{C}$; (a) $Re=1046$, $Bn=17.01$; (b) $Re=2092$, $Bn=8.5$.

As shown in Fig. 11, the increase in plastic viscosity $\mu_p(t)$ and the yield stress $\tau_0(t)$ in the low field causes a reduction in the maximum values of the velocity vector contour, compared to the previous case (see Fig. 7).

Fig. 12 demonstrates the radial profiles of axial velocity U and excess temperature θ at the inlet flow temperature of $t_1=25\text{ }^\circ\text{C}$, wall temperature of $t_w=10\text{ }^\circ\text{C}$, Reynolds number of $Re=1046$, and Bingham number of $Bn=17.01$ in a pipe with sudden enlargement.

The velocity U profiles tend to the shape of a Bingham fluid with a constant velocity core in the axial zone (see Fig. 12a). The excess temperature θ profiles are leveled at the regime parameters of $Re=1046$, $Bn=17.01$ (see Fig. 12b).

Fig. 13 illustrates the radial profiles of axial velocity U and excess temperature θ at the inlet flow temperature of $t_1=25\text{ }^\circ\text{C}$, wall temperature of $t_w=10\text{ }^\circ\text{C}$, Reynolds number of $Re=2092$, and Bingham number of $Bn=8.5$ in a pipe with a sudden enlargement.

At $Re=2092$ and $Bn=8.5$, the velocity U profile in the pipe section $x/R=10$ has a stagnation zone along the radius from $r/R=0.82$ to $r/R=1$. In further sections $x/R=20\div 40$, it has the

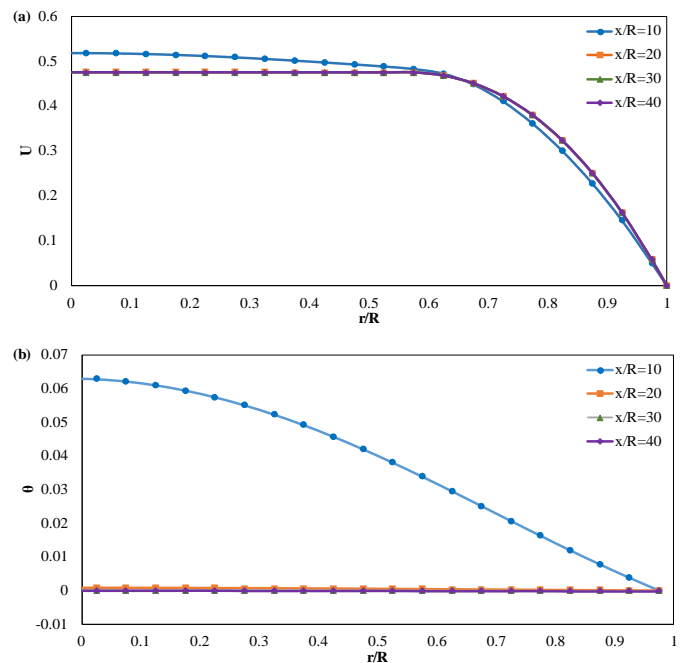


Fig. 12: Radial profiles of axial velocity U (a) and excess temperature θ (b) in a pipe with a sudden enlargement at operating parameters: $t_1=25\text{ }^\circ\text{C}$, $t_w=10\text{ }^\circ\text{C}$, $Re=1046$, $Bn=17.01$.

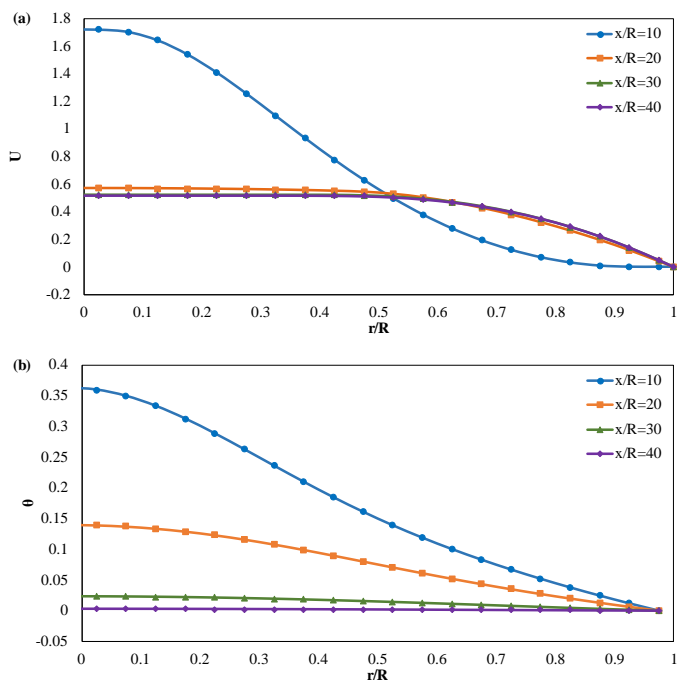


Fig. 13: Radial profiles of axial velocity U (a) and excess temperature θ (b) in a pipe with a sudden enlargement at operating parameters: $t_1=25\text{ }^\circ\text{C}$, $t_w=10\text{ }^\circ\text{C}$, $Re=2092$, $Bn=8.5$.

shape of a Bingham fluid flow (see Fig. 13a). The excess temperature θ profiles (Fig. 13b) show values slightly higher than those in the previous case (see Fig. 12b).

The pressure distributions along the pipe length with a sudden enlargement at the inlet flow temperature of $t_1=25\text{ }^\circ\text{C}$, wall temperature of $t_w=10\text{ }^\circ\text{C}$, Reynolds numbers of $Re=1046$ and $Re=2092$, and Bingham numbers of $Bn=17.01$ and $Bn=8.5$ are shown in Fig. 14.

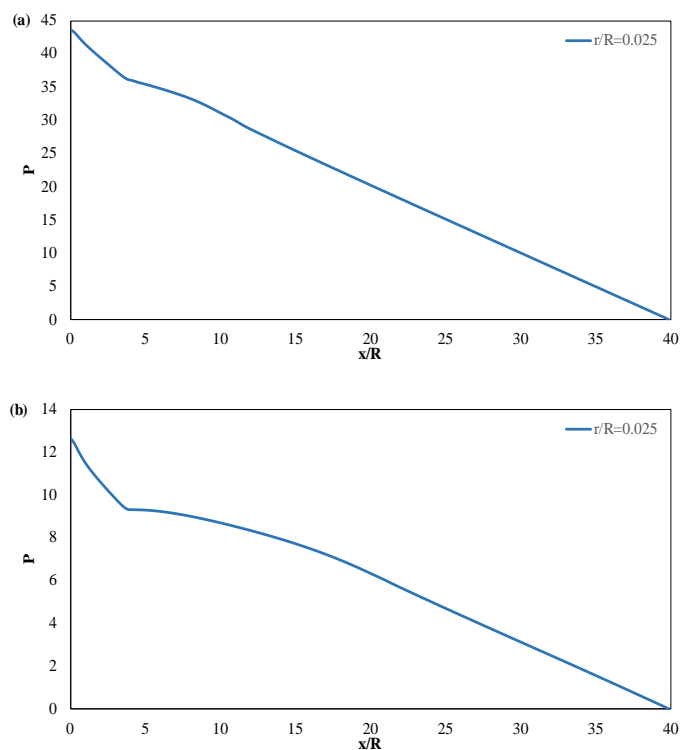


Fig. 14: Pressure distribution along the length of a pipe with a sudden enlargement at operating parameters: $t_1=25\text{ }^\circ\text{C}$, $t_w=10\text{ }^\circ\text{C}$; (a) $Re=1046$, $Bn=17.01$; (b) $Re=2092$, $Bn=8.5$.

4. Conclusion

Modeling of laminar flow and heat transfer of viscoplastic fluid is carried out in a pipe with a sudden enlargement. The numerical solution of the system of equations of motion and heat transfer is obtained by the control volume method in the variables "velocity components - pressure". In the isothermal flow, there is a reverse flow zone, which expands in length and width at the Reynolds numbers of $Re=1046$ and $Re=2092$ and Bingham numbers of $Bn=0.05$ and $Bn=0.025$. The pressure distributions along the pipe length have negative values due to the sudden enlargement of a pipe and the presence of a reverse flow zone. At the Reynolds number of $Re=2092$ and Bingham number of $Bn=0.025$, the pressure has a negative value up to the pipe section $x/R=35$ and is restored to the pipe outlet section $x/R=40$. In a non-isothermal flow with the Bingham numbers from $Bn=8.5$ to $Bn=59.14$, there is no reverse flow zone, i.e., the growth of the viscoplastic state of the fluid levels out the effect of the jump in the pipe cross-section. In this case, a stagnation zone appears where the flow velocity is zero. With the Bingham number of $Bn=29.59$ and the Reynolds number of $Re=2092$, the stagnation zone occupies a large area, starting from the pipe enlargement cross-section $x/R=4$ to the cross-section $x/R=25$. The calculated data established that an increase in the Reynolds number and a decrease in the Bingham number lead to an increase in the heat exchange in a pipe with a sudden enlargement. This is clearly shown for $Re=2092$ and $Bn=8.5$. The results of numerical simulation of viscoplastic fluid flow in a pipe with a sudden enlargement can also be applied to the flow of viscoplastic fluids in technical

devices used for casting metals, polymers, and ceramic slip products. Understanding the patterns of hydrodynamics and heat transfer in such flows is essential for ensuring the quality of the resulting products.

Acknowledgements

This work was supported by the Science Committee of the Ministry of Science and Higher Education of the Republic of Kazakhstan (Grant number BR20280990 for 2023-2025). The rheological model and their numerical realization were developed under the state contract with IT SB RAS (121031800217-8).

Conflict of Interest

There is no conflict of interest.

Supporting Information

Not applicable.

References

- [1] M. A. Habib, J. H. Whitelaw, The calculation of turbulent flow in wide-angle diffusers, *Numerical Heat Transfer, Part B: Fundamentals*, 1982, **5**, 145-164, doi: 10.1080/10407798208547011.
- [2] E. O. Macagno, T. K. Hung, Computational and experimental study of a captive annular eddy, *Journal of Fluid Mechanics*, 1967, **28**, 43-64, doi: 10.1017/s0022112067001892.
- [3] P. J. Oliveira, F. T. Pinho, Pressure drop coefficient of laminar Newtonian flow in axisymmetric sudden expansions, *International Journal of Heat and Fluid Flow*, 1997, **18**, 518-529, doi: 10.1016/S0142-727X(97)80010-0.
- [4] G. C. Vradis, M. V. O'tu'gen, The axisymmetric sudden expansion flow of a non-Newtonian viscoplastic fluid, *Journal of Fluids Engineering*, 1997, **119**, 193-200, doi: 10.1115/1.2819108.
- [5] P. Jay, A. Magnin, J. M. Piau, Viscoplastic fluid flow through a sudden axisymmetric expansion, *AIChE Journal*, 2001, **47**, 2155-2166, doi: 10.1002/aic.690471004.
- [6] M. Alghamdi, N. S. Akbar, T. Zamir, T. Muhammad, Double layered combined convective heated flow of Eyring-Powell fluid across an elevated stretched cylinder using intelligent computing approach, *Case Studies in Thermal Engineering*, 2024, **54**, 104009, doi: 10.1016/j.csite.2024.104009.
- [7] N. S. Akbar, J. Akram, M. F. Hussain, E. N. Maraj, T. Muhammad, Thermal storage study and enhancement of heat transfer through hybrid Jeffrey nanofluid flow in ducts under peristaltic motion with entropy generation, *Thermal Science and Engineering Progress*, 2024, **49**, 102463, doi: 10.1016/j.tsep.2024.102463.
- [8] N. S. Akbar, M. Rafiq, T. Muhammad, M. Alghamdi, Microbic flow analysis of nano fluid with chemical reaction in microchannel with flexural walls under the effects of thermophoretic diffusion, *Scientific Reports*, 2024, **14**, 1474, doi: 10.1038/s41598-023-50915-6.
- [9] M. A. Jamali, A. Bissenbay, N. Nuraje, Thermodynamic modeling and process simulation of kumkol crude oil refining,

- Eurasian Chemico-Technological Journal*, 2023, **25**, 183-192, doi: 10.18321/ectj1521.
- [10] P. R. de Souza Mendes, M. F. Naccache, P. R. Vargas, F. H. Marchesini, Flow of viscoplastic liquids through axisymmetric expansions–contractions, *Journal of Non-Newtonian Fluid Mechanics*, 2007, **142**, 207-217, doi: 10.1016/j.jnnfm.2006.09.007.
- [11] M. Bekhadra, N. S. Chemloul, A. Menouer, K. Chaib, Numerical study of laminar Bingham fluid in axisymmetric sudden expansion, *International Journal of Heat and Technology*, 2022, **40**, 45-52, doi: 10.18280/ijht.400106.
- [12] K. J. Hammad, G. C. Vradis, M. V. O'tu"gen, Laminar flow of a Herschel-bulkley fluid over an axisymmetric sudden expansion, *Journal of Fluids Engineering*, 2001, **123**, 588-594, doi: 10.1115/1.1378023.
- [13] K. J. Hammad, Suddenly expanding recirculating and non-recirculating viscoplastic non-Newtonian flows, *Journal of Visualization*, 2015, **18**, 655-667, doi: 10.1007/s12650-015-0279-9.
- [14] T. Hawa, Z. Rusak, Viscous flow in a slightly asymmetric channel with a sudden expansion, *Physics of Fluids*, 2000, **12**, 2257-2267, doi: 10.1063/1.1287610.
- [15] A. L. Forrest, K. P. Fattah, D. S. Mavinic, F. A. Koch, Optimizing struvite production for phosphate recovery in WWTP, *Journal of Environmental Engineering*, 2008, **134**, 395-402, doi: 10.1061/(asce)0733-9372(2008)134:5(395).
- [16] B. C. Bell, K. S. Surana, P-Version least squares finite element formulation for two-dimensional incompressible Newtonian and non-Newtonian non-isothermal fluid flow, *Computers & Structures*, 1995, **54**, 83-96, doi: 10.1016/0045-7949(94)E0280-F.
- [17] P. S. Scott, F. Mirza, J. Vlachopoulos, Finite-element simulation of laminar viscoplastic flows with regions of recirculation, *Journal of Rheology*, 1988, **32**, 387-400, doi: 10.1122/1.549976.
- [18] D. Badekas, D. D. Knight, Eddy correlations for laminar axisymmetric sudden expansion flows, *Journal of Fluids Engineering*, 1992, **114**, 119-121, doi: 10.1115/1.2909986.
- [19] İ. Dağtekin, M. Ünsal, Numerical analysis of axisymmetric and planar sudden expansion flows for laminar regime, *International Journal for Numerical Methods in Fluids*, 2011, **65**, 1133-1144, doi: 10.1002/flid.2239.
- [20] S. Mishra, K. Jayaraman, Asymmetric flows in planar symmetric channels with large expansion ratio, *International Journal for Numerical Methods in Fluids*, 2002, **38**, 945-962, doi: 10.1002/flid.242.
- [21] R. Manica, A. L. De Bortoli, Simulation of sudden expansion flows for power-law fluids, *Journal of Non-Newtonian Fluid Mechanics*, 2004, **121**, 35-40, doi: 10.1016/j.jnnfm.2004.03.009.
- [22] F. T. Pinho, P. J. Oliveira, J. P. Miranda, Pressure losses in the laminar flow of shear-thinning power-law fluids across a sudden axisymmetric expansion, *International Journal of Heat and Fluid Flow*, 2003, **24**, 747-761, doi: 10.1016/S0142-727X(03)00083-3.
- [23] D. A. Mamazova, K. E. Ryltseva, G. R. Shrager, The structure and kinematics of a non-newtonian fluid flow in a pipe with a sudden expansion, *Tomsk State University Journal of Mathematics and Mechanics*, 2021, **74**, 113-126, doi: 10.17223/19988621/74/12.
- [24] G. C. Vradis, K. J. Hammad, Heat transfer in flows of non-Newtonian Bingham fluids through axisymmetric sudden expansions and contractions, *Numerical Heat Transfer, Part A: Applications*, 1995, **28**, 339-353, doi: 10.1080/10407789508913749.
- [25] K. J. Hammad, G. C. Vradis, Creeping flow of a Bingham plastic through axisymmetric sudden contractions with viscous dissipation, *International Journal of Heat and Mass Transfer*, 1996, **39**, 1555-1567, doi: 10.1016/0017-9310(95)00273-1.
- [26] K. J. Hammad, The effect of hydrodynamic conditions on heat transfer in a complex viscoplastic flow field, *International Journal of Heat and Mass Transfer*, 2000, **43**, 945-962, doi: 10.1016/S0017-9310(99)00179-9.
- [27] K. J. Hammad, Inertial thermal convection in a suddenly expanding viscoplastic flow field, *International Journal of Heat and Mass Transfer*, 2017, **106**, 829-840, doi: 10.1016/j.ijheatmasstransfer.2016.10.013.
- [28] K. E. Ryltseva, E. I. Borzenko, G. R. Shrager, Non-Newtonian fluid flow through a sudden pipe contraction under non-isothermal conditions, *Journal of Non-Newtonian Fluid Mechanics*, 2020, **286**, 104445, doi: 10.1016/j.jnnfm.2020.104445.
- [29] H. A. Barnes, The yield stress: a review or 'παντα ρει': everything flows? *Journal of Non-Newtonian Fluid Mechanics*, 1999, **81**, 133-178, doi: 10.1016/S0377-0257(98)00094-9.
- [30] E. C. Bingham, Fluidity and Plasticity, 1922.
- [31] W. L. Wilkinson, Non-newtonian fluids. Fluid mechanics, mixing and heat transfer, 1960.
- [32] T. C. Papanastasiou, Flows of materials with yield, *Journal of Rheology*, 1987, **31**, 385-404, doi: 10.1122/1.549926.
- [33] U. Zhapbasbayev, T. Bekibayev, M. Pakhomov, G. Ramazanova, Numerical modeling of non-isothermal laminar flow and heat transfer of paraffinic oil with yield stress in a pipe, *Energies*, 2024, **17**, 2080, doi: 10.3390/en17092080.
- [34] S. Patankar, Numerical heat transfer and fluid flow, 1980.
- [35] E. Mitsoulis, R. R. Huilgol, Entry flows of Bingham plastics in expansions, *Journal of Non-Newtonian Fluid Mechanics*, 2004, **122**, 45-54, doi: 10.1016/j.jnnfm.2003.10.007.

Publisher's Note: Engineered Science Publisher remains neutral with regard to jurisdictional claims in published maps and institutional affiliations.

Open Access

This article is licensed under a Creative Commons Attribution 4.0 International License, which permits the use, sharing, adaptation, distribution and reproduction in any medium or format, as long as appropriate credit to the original author(s) and the source is given by providing a link to the Creative Commons licence and changes need to be indicated if there are

any. The images or other third-party material in this article are included in the article's Creative Commons licence, unless indicated otherwise in a credit line to the material. If material is not included in the article's Creative Commons licence and your intended use is not permitted by statutory regulation or exceeds the permitted use, you will need to obtain permission directly from the copyright holder. To view a copy of this licence, visit <http://creativecommons.org/licenses/by/4.0/>.

©The Author(s) 2025